



## Real-time mass spectroscopy analysis of Li-ion battery electrolyte degradation under abusive thermal conditions

B. Gaulupeau, B. Delobel, S. Cahen, S. Fontana, Claire Hérold

### ► To cite this version:

B. Gaulupeau, B. Delobel, S. Cahen, S. Fontana, Claire Hérold. Real-time mass spectroscopy analysis of Li-ion battery electrolyte degradation under abusive thermal conditions. *Journal of Power Sources*, 2017, 342, pp.808-815. 10.1016/j.jpowsour.2016.12.078 . hal-02352028

HAL Id: hal-02352028

<https://hal.univ-lorraine.fr/hal-02352028v1>

Submitted on 9 Feb 2022

**HAL** is a multi-disciplinary open access archive for the deposit and dissemination of scientific research documents, whether they are published or not. The documents may come from teaching and research institutions in France or abroad, or from public or private research centers.

L'archive ouverte pluridisciplinaire **HAL**, est destinée au dépôt et à la diffusion de documents scientifiques de niveau recherche, publiés ou non, émanant des établissements d'enseignement et de recherche français ou étrangers, des laboratoires publics ou privés.

# Real-time mass spectroscopy analysis of Li-ion battery electrolyte degradation under abusive thermal conditions

B. Gaulupeau<sup>1,2</sup>, B. Delobel<sup>2</sup>, S. Cahen<sup>1</sup>, S. Fontana<sup>1</sup>, C. Hérold<sup>1</sup>

<sup>1</sup>Institut Jean Lamour, UMR 7198 CNRS-Université de Lorraine, Faculté des Sciences et Technologies, BP 70239, 54506 Vandœuvre-lès-Nancy cedex, France.

<sup>2</sup>Technocentre Renault, 1 avenue du Golf, 78288 Guyancourt, France.

## Abstract

The lithium-ion batteries are widely used in rechargeable electronic devices. The current challenges are to improve the capacity and safety of these systems in view of their development to a larger scale, such as for their application in electric (EVs) and hybrid (HEVs) vehicles. Lithium-ion batteries use organic solvents because of the wide operating voltage. The corresponding electrolytes are usually based on combinations of linear, cyclic alkyl carbonates and a lithium salt such as LiPF<sub>6</sub>. It has been reported that in abusive thermal conditions, a catalytic effect of the cathode materials lead to the formation fluoro-organics compounds. In order to understand the degradation phenomenon, the study at 240°C of the interaction between positive electrode materials (LiCoO<sub>2</sub>, LiNi<sub>1/3</sub>Mn<sub>1/3</sub>Co<sub>1/3</sub>O<sub>2</sub>, LiMn<sub>2</sub>O<sub>4</sub> and LiFePO<sub>4</sub>) and electrolyte in dry and wet conditions has been realized by an original method which consists in analyzing by mass spectrometry in real time the volatile molecules produced. The evolution of specific gases channels coupled to the NMR reveal the formation of rarely discussed species such as 2-fluoroethanol and 1,4-dioxane. Furthermore, it appears that the presence of water or other protic impurities greatly influence their formation.

## Keywords

lithium-ion battery; electrolyte; cathode materials; safety; mass spectrometry

## Introduction

The use of lithium-ion batteries has been democratized thanks to its larger energy density than other storage technologies. For instance, it is involved in large-scale infrastructures or integrated in electric vehicles [1]. In the latter case, the high power and energy densities involved require special attention concerning the safety of such systems, so that the management of these batteries and their safety are key points.

Numerous papers in the literature deal with the behavior of the Solid Electrolyte Interphase (SEI) formed at the negative electrode-electrolyte interface. Indeed, the rupture of the SEI, exposing the charged anode to the electrolyte lead to its reduction (solvent and lithium salt) accompanied by local exothermic reactions [2]. This increase of temperature can then be spread to the whole Li-ion device, until the manifestation of a thermal runaway [3]. Such an incident must be carefully considered as it may reject different gaseous species (hydrocarbons, carbon oxides, fluoro-organic molecules, ...) [4]. In fact, the nature of the emitted gases depends on the combination of electrode materials and electrolyte.

The electrolyte is generally composed of a mixture of linear and cyclic carbonates with lithium salt. It consists in the most vulnerable component of the battery, that is why its electrochemical and/or thermal stability is still currently carefully checked [5]. Moreover, this problematic is clearly of interest as various combinations of lithium salts and solvents can be considered.

Among them, 1 M LiPF<sub>6</sub> EC/DMC (1:1, w/w) (LP30) is a commonly studied electrolyte in the literature. Even if it is characterized by a good electrochemical stability and high conductivity, it

presents the drawback of the poor thermal stability of LiPF<sub>6</sub> at the relatively low temperature range [380-467K] [6, 7], following the thermolysis reaction recently confirmed by [8, 9]:

Eq. 1



Moreover, phosphorous pentafluoride or neat LiPF<sub>6</sub> can also react with traces of moisture:



In all cases, the formed decomposition products (PF<sub>5</sub>, OPF<sub>3</sub>, HF) can then decompose the solvent to form a large variety of degradation species depending on thermal conditions, but an exhaustive list of molecules cannot be easily established. Various thermal analyses have been performed (differential scanning calorimetry (DSC), accelerating rate calorimetry (ARC), thermogravimetric analyses (TGA)) in a wide range of experimental conditions, and the reader can retrieve further information in [10, 8, 11, 12, 13]. Other papers put their interest in the nature of the produced species under 85°C using gas chromatography coupled with mass spectrometry (GC-MS) [14, 15], Fourier transform infrared spectroscopy (FT-IR) [16] or nuclear magnetic resonance (NMR) [17]. In the past few years research has deployed much effort to find new techniques for the investigation of electrolyte degradation. It mostly relies on coupled techniques such as ionic chromatography-mass spectrometry (IC-MS), electrospray ionization-mass spectrometry (ESI-MS), inductively coupled plasma optical emission spectrometry (ICP-OES), low-temperature plasma probe high resolution mass spectrometry (LTP-HRMS) [18, 19, 20, 21]. The main reactions taking place during thermolysis or hydrolysis of LiPF<sub>6</sub> are always in agreement with Eq.1-3. Moreover, the nature of gaseous species formed at higher temperature (*i.e.* in abusive thermal conditions when the beginning of a thermal runaway occurs) has not been deeply investigated.

As mentioned before, in case of thermal runaway, all the components of the battery are involved. If numerous papers have been published concerning the thermal behavior of the electrolyte alone [11, 22, 23] or in contact with negative electrode material, only a few works concern the phenomena occurring between electrolyte and the positive electrode material in case of rise of the temperature [24, 25, 26]. Nevertheless, it can be interesting to be focused on the nature of the degradation products at the positive electrode interface which have been very few studied [17, 27]. In this field of research, the paper of Hamami *et al.* should be emphasized [27]. These authors have studied by a step-by-step approach the emitted gases for various solvent-lithium salts mixtures heated at 240°C for 30-60 minutes. They mention the abundant formation of various fluoro-organics when LiPF<sub>6</sub>-EC electrolyte is in contact with LiCoO<sub>2</sub> and highlighted the preponderant role of ethylene carbonate for the production of fluoro-organic molecules, whereas the presence of DMC decreases the yield of formation of such substances. However, a yield of 80% corresponding to fluoro-organics is announced without any details.

During our study, we decided to rule out LP30 in order to be only focused on a simplified reference electrolyte. Moreover, the purpose of our work is to develop an *in situ* technique able to probe electrolyte degradation in abusive thermal conditions leading to the beginning of a thermal runaway. In fact, most of the studies investigate degradation products with long term ageing (from 24h to few weeks) or with a full simulation of thermal runaway that produces mostly combustion products [28, 29, 30]. Contrarily, Hamami *et al* [27] who highlighted the formation of fluoro-organics molecules studied under intermediate thermal conditions corresponding to the beginning of a thermal runaway.

That's why this paper is focused on the determination of nature of the formed gaseous species when different cathode materials LiCoO<sub>2</sub> (LCO), LiNi<sub>1/3</sub>Mn<sub>1/3</sub>Co<sub>1/3</sub>O<sub>2</sub> (NMC), LiMn<sub>2</sub>O<sub>4</sub> (LMO), LiFePO<sub>4</sub>(LFP) are in contact with the EC-LiPF<sub>6</sub> 1M electrolyte at 240°C during 100 minutes. Concerning the detection of the possible formed fluoro-organic molecules, the device developed in this work is particularly adapted to the detection of 2-fluoroethanol. Its detection would imply that, considering the work of Hammami *et al.* [27], other fluoro-organic molecules could also be formed. However; they have not been tracked in the present work as it would necessitate additional analytical developments. The influence of traces of moisture has also been investigated in these conditions. In order to study this system, an original real-time mass spectrometry set-up has been developed. The original technique developed during this study aims to follow individually the effect of each positive electrode material that can be involved in a Li-ion battery. To proceed, the study is first realized on a simplified reference electrolyte. Then, the latter is mixed with different active materials. Finally, the influence of water in such mixtures is also probed.

## 2. Experimental

LCO, NMC, LMO and coated LFP (C-LFP) cathode materials have been obtained by several providers. The cathode materials are used as powders, what ensure a better contact between active material and electrolyte. The reactivity will so be increased, what lead to an easier detection of the degradation products. The samples are powder presenting equivalent controlled grain size going from 5 µm to 30 µm with a specific surface going from 0.2 to 0.4 m<sup>2</sup>.g<sup>-1</sup>, corresponding to similar textures. Thermogravimetric analyses (TGA) show the presence of traces of physisorbed water on all powders, that is why each powder has been outgassed (250°C for 7h under 2<sup>ry</sup> vacuum). Then, samples are consecutively controlled by TGA (showing absence of residual physisorbed water), and X-ray diffraction (XRD) experiments confirming that no structural modification of the materials occurred (results not shown).

Electrolyte preparation: LiPF<sub>6</sub> (Acros, 98%) was used after being outgassed under secondary vacuum (10<sup>-6</sup> mbar) at 100°C, and ethylene carbonate (EC - Sigma Aldrich, 99%) was used without further purification. As mentioned, Hammami *et al.* [27] studied an electrolyte that consists in a mixture of LiPF<sub>6</sub> and ethylene carbonate. According to these authors, the main fluorinated degradation products are formed from EC. Moreover, it appears that linear carbonate such as dimethyl carbonate (DMC) shows a high volatility problematic while using mass spectrometry. Indeed, its fragmentation pattern consists in numerous light fragments that may hide the expected fragments coming from other molecules. For all these reasons, DMC has been removed from the working electrolyte.

Even if we are taking numerous precautions in order to avoid any contamination by moisture (working under controlled atmosphere), it should be noted that ethylene carbonate used as solvent could anyway contain traces of water (less than 20 ppm) [31]. In this study, LiPF<sub>6</sub> is dissolved into EC and heated at 40°C overnight under inert nitrogen atmosphere and the so-obtained mixture is considered as the simplified reference electrolyte (dry conditions). When studying the impact of water on the degradation mechanisms, the amount of controlled added water is systematically 1000 ppm and the used denomination is "wet conditions".

*In situ* mass spectrometry (MS) has been carried out using a reactor directly connected to the mass spectrometer (Prisma<sup>TM</sup> device from Pfeiffer vacuum). A set of bubbler and valves is used to control the pressure in the entire device (atmospheric pressure), helium being used as a carrier gas. Cathode material-electrolyte mixtures were heated from room temperature to 240°C with a heating rate of 30°C.min<sup>-1</sup>. The isotherm is reached after 8 minutes and the

measurements last a total of 100 minutes. These thermal conditions have been selected mainly in order to compare our results with those of Hammami *et al.* [27], and considering the boiling point of EC (245°C). In this study, the isothermal analysis at 240°C is investigated in order to probe the behavior of the simplified reference electrolyte in abusive thermal conditions, equivalent to the beginning of a thermal runaway.

Protocol of *in situ* MS is as follow: around 200 mg of positive electrode material is weighted in a glove box (under purified argon) then immersed in 3 g of electrolyte. The reactor is filled with the powder and the electrolyte, before being isolated and transferred to the system. Before starting the experiment, helium ( $\text{H}_2\text{O} < 0.5\text{ppm}$ ,  $\text{O}_2 < 0.1\text{ppm}$ ) is flushed for 2 hours to purge the transfer line ensuring that the mixture is not contaminated. The bubbler allows to check the flow rate and keep an atmospheric pressure into the system. Then, 2 micrometric valves allow to control the input pressure reaching the mass spectrometer which will be directly open to the system. Compounds identification (and corresponding formulae) was realized using the National Institutes of Standards (NIST) library as a reference. For indexation, on one hand the analysis is focused on the most intense fragment and on another hand on the presence of the characteristic molecular ion peak even if its intensity is low. It should be noted that no chromatographic device is involved in this apparatus.

When possible, *ex situ* NMR measurements are also performed in order to confirm some of the proposed degradation products deduced from experiments.

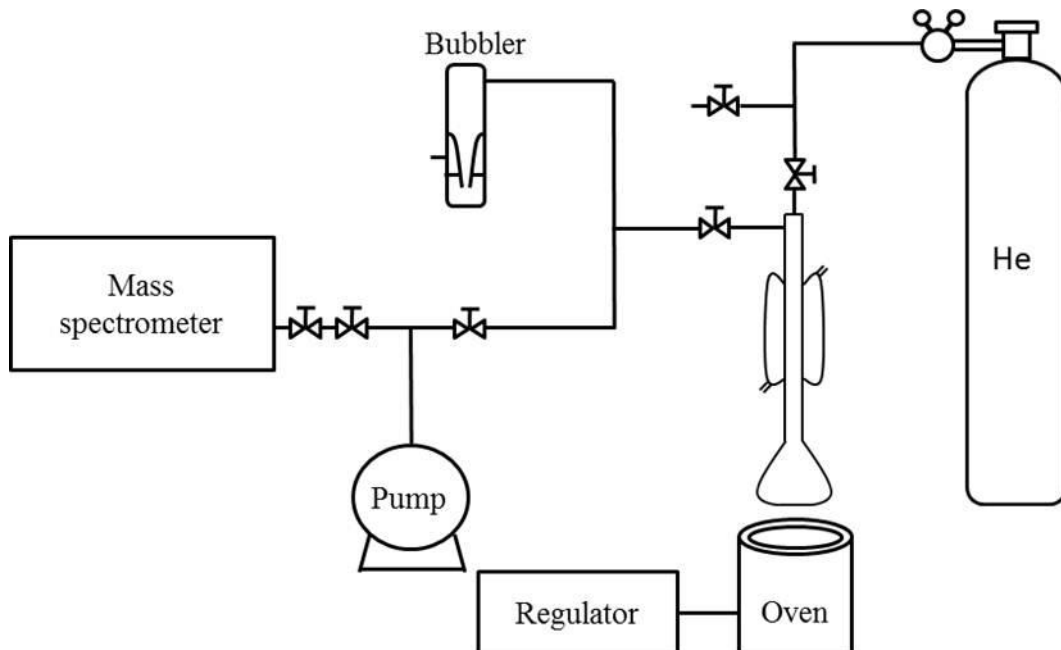


**Figure 1:** Schematic illustration of the *in situ* MS device.

Nuclear magnetic resonance (NMR) measurements were performed using a Brucker Advance III 400 and a BBFO (Broad Band Fluorine Observation) probe. The magnetic field is 9.4T corresponding to a resonance frequency of 400 MHz. The product has been dissolved in  $\text{CDCl}_3$  (Sigma Aldrich 99.8 atom % D). The  $^{19}\text{F}$  chemical shift spectra were recorded with the following parameters: spectral width (250 ppm), offset (-150 ppm), scan number (2048 scans), data points (128k), relaxation time (1s). The  $^1\text{H}$  chemical shift spectra were recorded with the following parameters: spectral width (20 ppm), scan number (16 scans), data points (64k), relaxation time (1s).

### 3. Results and discussion

#### 3.1 In situ mass spectroscopy of the EC-LiPF<sub>6</sub> system

It is now well accepted that LiPF<sub>6</sub> can decompose from thermolysis into PF<sub>5</sub> and LiF, and into OPF<sub>3</sub>, LiF and HF from hydrolysis, what has been confirmed using especially TGA-FTIR [6, 16, 32]. Considering eq. 2-3, it has been possible to detect HF thanks to *in situ* mass spectroscopy in this study, with a nice correlation between the m/z = 19 and m/z = 20 (HF<sup>+</sup> molecular ion) signals. Contrarily, PF<sub>5</sub> is not detected, what is easily explained considering the high reactivity of pentafluoride phosphorous towards electrolyte. Figure 2 shows the two characteristic fragments of gaseous HF (F<sup>+</sup> and HF<sup>+</sup>) together with the 3 main fragments of gaseous OPF<sub>3</sub> (OPF<sub>3</sub><sup>+</sup>, OPF<sub>2</sub><sup>+</sup>, OPF<sup>+</sup>).

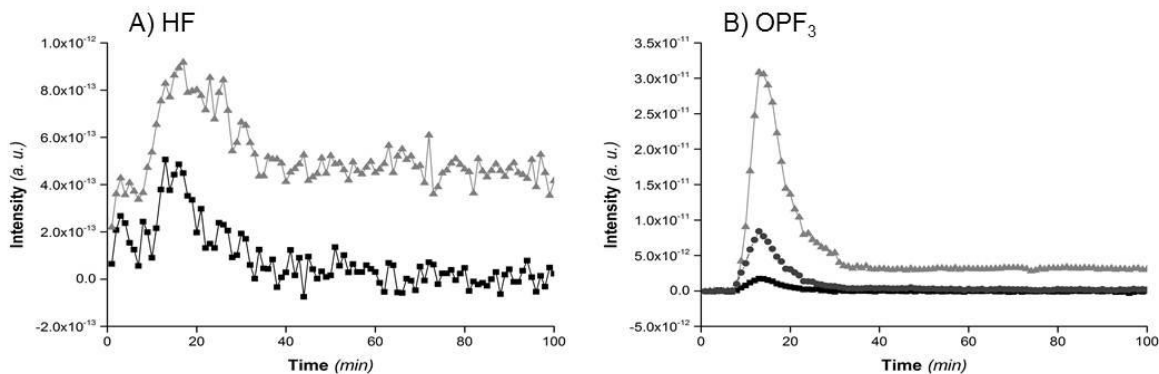


**Figure 2:** A) Evolution of the F<sup>+</sup>(■), HF<sup>+</sup>(▲) fragments (channels 19 and 20) characteristic of HF and B) PF<sub>2</sub><sup>+</sup>(■), OPF<sub>2</sub><sup>+</sup>(▲), OPF<sub>3</sub><sup>+</sup>(●) fragments (channels 69, 85 and 104) characteristic of OPF<sub>3</sub>.

After a maximum of volatilization for 10-15 minutes heating (thermalizing of the reactor at 240°C), no more fluorinated product is detected. The detection of these species means that even in dry conditions hydrolysis takes place due to traces of water/protic impurities (from helium flow or solvent). It is assumed that thermolysis takes place first, before that produced PF<sub>5</sub> gas hydrolyses into OPF<sub>3</sub>.

It should be noted that, due to the glassy nature of the used reactor, the HF formation can also indirectly be checked by *in situ* MS due to the SiF<sub>4</sub> formation [33] following:



Here we emphasize that some authors have already worked in presence of fluorinated species using glass ampoule [17], and even checked the impact of the presence of SiO<sub>2</sub> which can be found with glass fiber separator [21, 34]. The different authors stated on the fact that the reaction with SiO<sub>2</sub> would exacerbate degradation phenomena, but without the formation of new species.

As chemical species can present mutual m/z fragments simultaneously (for instance m/z = 85 for OPF<sub>2</sub><sup>+</sup> and SiF<sub>3</sub><sup>+</sup>), some molecules can hardly be identified by MS considering one unique channel. It is so necessary to focus on other m/z channels corresponding to secondary fragments. Considering the possible confusion between OPF<sub>3</sub> and SiF<sub>4</sub> molecules using the m/z = 85 channel, the OPF<sub>3</sub><sup>+</sup> fragment (m/z = 104, denoted molecular ion whose presence is

very important in order to discriminate the two molecules, Figure 2B) and the  $^{29}\text{SiF}_3^+$  and  $^{30}\text{SiF}_3^+$  fragments ( $m/z = 86$  and  $87$  respectively) are taken into account to confirm the  $\text{OPF}_3$  and  $\text{SiF}_4$  molecules emission. In the following study, the  $\text{SiF}_4$  emission will not be discussed (but not neglected as it is an indirect indication of the HF formation) in order to be only focused on the gas emissions due to reactions taking place in the reactor (see supplementary materials).

The thermal degradation of the electrolyte leads to different decomposition products detected by mass spectrometry (Figure 3).

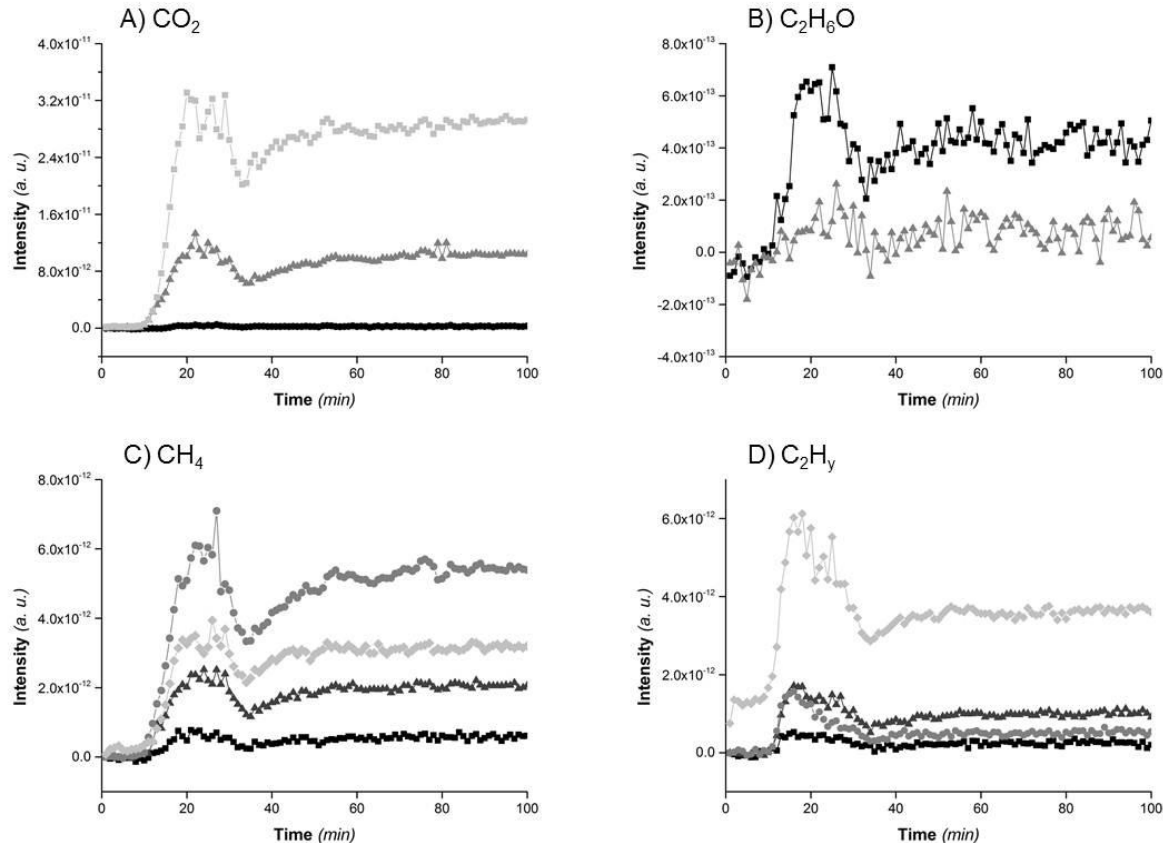
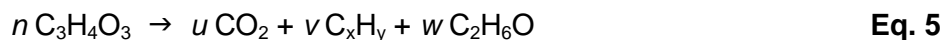


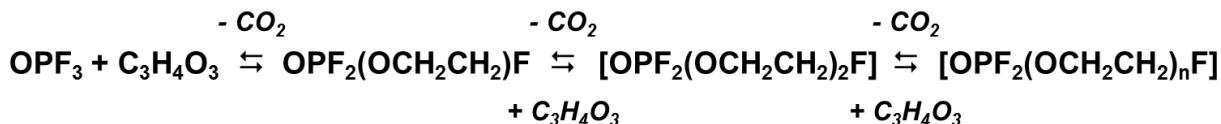
**Figure 3:** Evolution of the:  
 A)  $\text{CO}_2^{++}$  (●),  $\text{CO}^+$  (▲),  $\text{CO}_2^+$  (■) fragments (channels 22, 29 and 44) characteristic of  $\text{CO}_2$ ,  
 B)  $\text{C}_2\text{H}_5\text{O}^+$  (■),  $\text{C}_2\text{H}_6\text{O}^+$  (▲) fragments (channels 45 and 46) characteristic of  $\text{C}_2\text{H}_6\text{O}$ ,  
 C)  $\text{CH}^+$  (■),  $\text{CH}_2^+$  (▲),  $\text{CH}_3^+$  (●),  $\text{CH}_4^+$  (◇) fragments (channels 13, 14, 15 and 16) characteristic of  $\text{CH}_4$ ,  
 D)  $\text{C}_2\text{H}^+$  (■),  $\text{C}_2\text{H}_2^+$  (▲),  $\text{C}_2\text{H}_3^+$  (●),  $\text{C}_2\text{H}_4^+$  (◇) fragments (channels 25, 26, 27 and 28) characteristic of  $\text{C}_2\text{H}_y$ .

Different lightweight gases are detected and attributed to  $\text{CO}_2$  (Figure 3A), dimethyl ether (Figure 3B), and hydrocarbons  $\text{CH}_4$  and  $\text{C}_2\text{H}_y$  (Figure 3C-D). These gases come from the direct decomposition of the solvent (EC) following the reaction pathway:



All these products appear consecutively to the thermalizing of the reactor and the  $\text{OPF}_3$  and HF generation. They present a maximum of intensity recorded around 20 minutes before to decrease, but remain present with low intensity until the end of the experiment.

Another interesting information coming from *in situ* MS analysis is the high intensity of the signals due to the different fragments of the  $\text{CO}_2$  molecule (Figure 3A). This may indicate that several compounds are decomposing into  $\text{CO}_2$ . Campion *et al.* have shown that a polymerization mechanism occurs during the thermal degradation of the EC-LiPF<sub>6</sub> mixture [17]. This mechanism is a reaction between  $\text{OPF}_3$  and EC which produces  $[\text{OPF}_2(\text{OCH}_2\text{CH}_2)_n\text{F}]$  polymers accompanied at each step by the loss of a  $\text{CO}_2$  molecule as depicted in scheme 1.



**Scheme 1:** polymerization mechanism of EC

The aforementioned mechanism is in agreement with this study as we detect a large emission of  $\text{CO}_2$ . Moreover, we have investigated and confirmed the fluorinated polymers formation thanks to <sup>19</sup>F NMR (Figure 4).

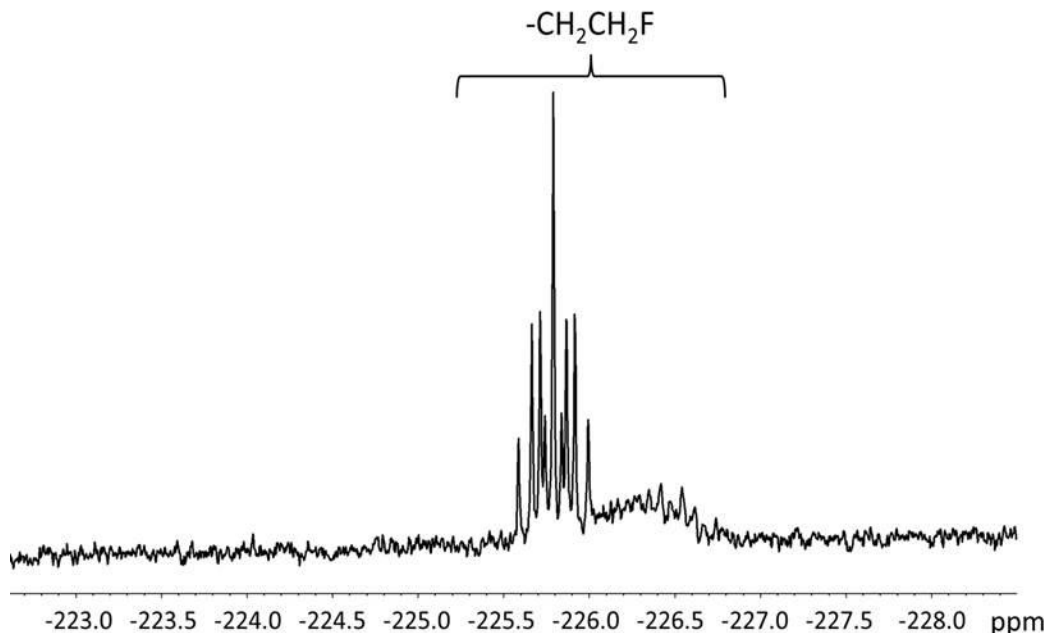


**Figure 4:** <sup>19</sup>F NMR spectrum area of R-CH<sub>2</sub>CH<sub>2</sub>F in EC-LiPF<sub>6</sub> system.

The two multiplets between -225.5 ppm and -227 ppm are attributed to R-CH<sub>2</sub>CH<sub>2</sub>F and consistent with -CH<sub>2</sub>CH<sub>2</sub>F termination of the  $[\text{OPF}_2(\text{OCH}_2\text{CH}_2)_n\text{F}]$  polymers identified by Gnanaraj *et al.* [11]. It is believed that the signal centered at -225.55 ppm correspond to the n=1 polymer and the poorly resolved signal centered at -226.5 ppm to the n=2 polymer.

### 3.2. Influence of the positive electrode material on the decomposition of EC-LiPF<sub>6</sub> electrolyte

Considering the work of Hammami *et al.* [27] who claim that the yield of fluoro-organic compounds depends on the presence of  $\text{LiCoO}_2$  in the EC-LiPF<sub>6</sub> electrolyte, we have investigated the influence of the cathode material on the way of decomposition occurring in the reactive medium. This study is focused on both LCO and NMC compounds (layered materials), and also on LMO (spinel) and C-LFP (olivine) as potential catalysts of the degradation phenomena. The cathode material is added to the electrolyte heated at 240 °C, and the decomposition is followed thanks to the CO<sub>2</sub> evolution (Figure 5) as it can be considered as a witness of EC degradation.

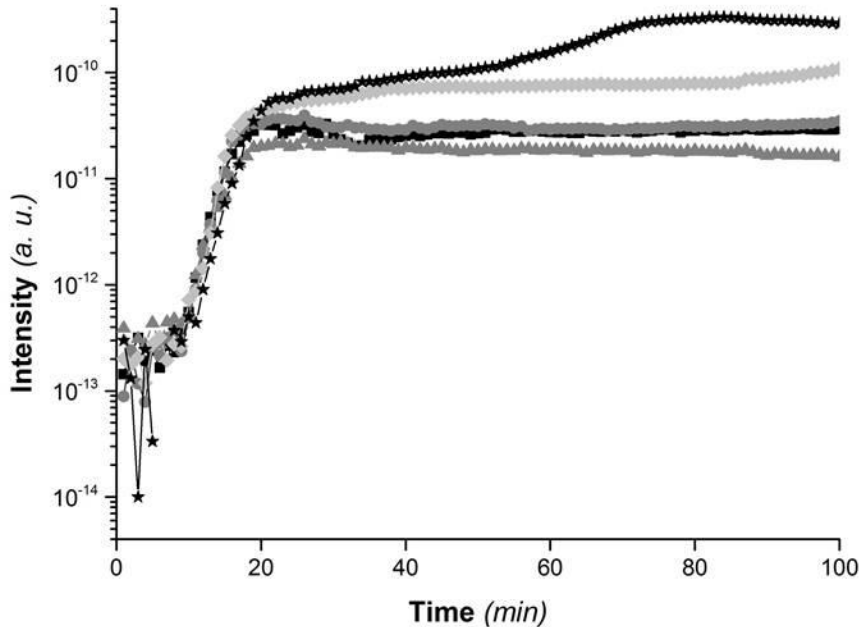


**Figure 5:** Logarithmic evolution of the CO<sub>2</sub><sup>+</sup> fragments (channel m/z = 44) characteristic of CO<sub>2</sub> from electrolyte alone (■); with: LCO(●), NMC(▲), LMO(◊), LFP(★).

The evolution of the CO<sub>2</sub> emission during the experiment is similar for electrolyte alone than for the LCO and NMC lamellar positive electrode material immersed in the EC-LiPF<sub>6</sub> electrolyte. On the contrary, the presence of LMO or C-LFP in the electrolyte leads to a higher intensity signal due to CO<sub>2</sub>, with significant differences especially for C-LFP which is one order of magnitude higher than other lamellar materials.

On the one hand, the addition of LMO leads to an increase of the detected quantity of CO<sub>2</sub> without any other significant modification. This increase is attributed to the combustion of EC into CO<sub>2</sub> as it is well known that LiMn<sub>2</sub>O<sub>4</sub> releases a significant amount of O<sub>2</sub> [35].

On the other hand, the addition of C-LFP leads to a more important CO<sub>2</sub> production. Although LiFePO<sub>4</sub> is recognized for its nice thermal stability, the abusive conditions used here suggest that the material is more vulnerable than its fellows [36]. Moreover, it is assumed that a possible decomposition of the carbon coating of the C-LFP active material may contributes to generate additional CO<sub>2</sub>. Further experiments will be performed in order to check the evolution of the carbon coating after thermal degradation.

In dry conditions, whatever is the active material, the decomposition of ethylene carbonate is systematically observed following eq.5. If LMO or C-LFP is involved, a greater reactivity versus

ethylene carbonate is observed with an increase of the amount of produced CO<sub>2</sub>. The list of the systematically detected molecules is as followed: C<sub>x</sub>H<sub>y</sub>, CO/CO<sub>2</sub>, dimethyl ether C<sub>2</sub>H<sub>6</sub>O, HF, OPF<sub>3</sub>. Elsewhere, no modification of the LiPF<sub>6</sub> decomposition has been pointed out whatever is the considered material and no new degradation molecule is detected, meaning that cathode materials do not present any catalytic effect on degradation reactions. In all cases, no fluoro-organic molecule is detected except in presence of C-LFP. In the latter case, the increased of the electrolyte degradation showed Figure 5 is accompanied with the potential detection (low intensity) of 2-fluoroethanol in a very small amount.

### 3.3. Influence of water on the decomposition of EC-LiPF<sub>6</sub> electrolyte

Considering that our study does not show the formation fluoro-organic compounds when LiPF<sub>6</sub>-EC electrolyte is heated together with LCO, we have investigated the influence of water in the electrolyte when the latter is thermally degraded. Indeed, a hydrolysis step is necessary in the mechanism proposed by Bergmann *et al.* [37].

When such a mixture is heated, a first indication of hydrolysis reaction (eq.2-3) is the detection of the F<sup>+</sup> and HF<sup>+</sup> fragments (Figure 6A) with one order of magnitude higher than with the simplified reference electrolyte. This increased formation of HF obviously leads to enhanced SiF<sub>4</sub> formation, what is not discussed as it does not seem to affect decomposition phenomena of the electrolyte. Another information arises from this measurement: after 40 minutes, the behavior of the F<sup>+</sup> fragment differs considering the different wet or dry conditions. This implies that other fluorinated species is formed in wet conditions but not yet identified.

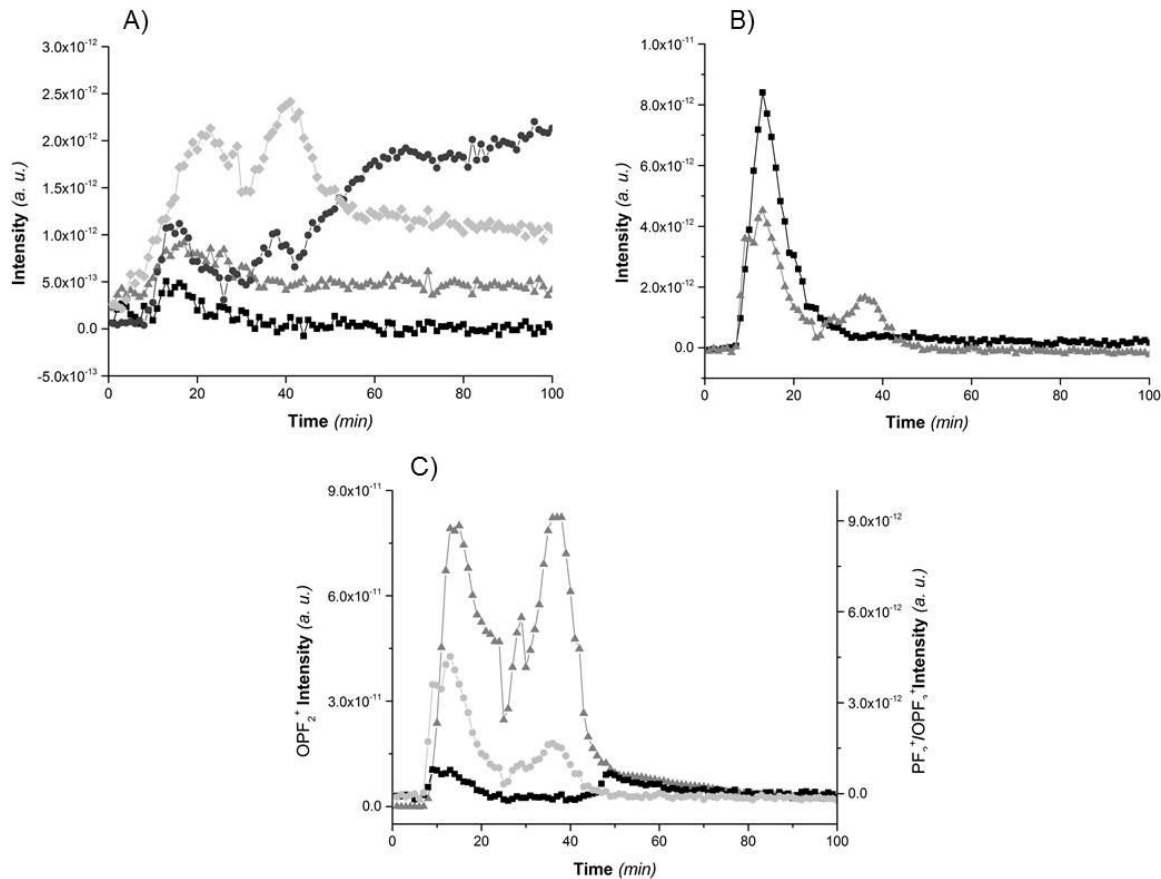


**Figure 6:** Evolution of the : A)  $\text{F}^+$ ,  $\text{HF}^+$  fragments (channels 19 and 20) characteristic of HF from EC-LiPF<sub>6</sub> (**■ and ▲**) and EC-LiPF<sub>6</sub>-H<sub>2</sub>O (**● and ◇**) systems.  
 B) OPF<sub>3</sub><sup>+</sup> molecular ion (channel 104) from EC-LiPF<sub>6</sub> (**■**) and EC-LiPF<sub>6</sub>-H<sub>2</sub>O (**▲**).  
 C) PF<sub>2</sub><sup>+</sup> (**■**), OPF<sub>2</sub><sup>+</sup> (**▲**), OPF<sub>3</sub><sup>+</sup> (**●**) fragments (channels 69, 85 and 104) attributed to OPF<sub>3</sub> from EC-LiPF<sub>6</sub>-H<sub>2</sub>O system.

Moreover, it is interesting to focus on signals recorded for the molecular ion OPF<sub>3</sub><sup>+</sup> ( $m/z = 104$ ) in dry and wet conditions (Figure 6B).

It clearly appears that OPF<sub>3</sub> is more intensively detected in dry conditions. Contrarily, the presence of water in the electrolyte leads to a decrease of the OPF<sub>3</sub> amount at the beginning of the experiment (before 20 minutes). This difference is easily explained by a possible hydrolysis of OPF<sub>3</sub> which occurs quickly, with simultaneous production of HF (figure 6A), OPF<sub>2</sub>OH, OPF(OH)<sub>2</sub> and H<sub>3</sub>PO<sub>4</sub> following eq.6-8:



In wet conditions, a second emission peak of OPF<sub>3</sub> is detected after 30 minutes of thermal degradation, what is highlighted Figure 6C by the simultaneous record of the  $m/z$  channels attributed to OPF<sub>3</sub>.

A regeneration of OPF<sub>3</sub> has been proposed by [17] and takes into consideration the reaction between linear carbonates and OPF<sub>3</sub> whereas in this study, cyclic ethylene carbonate is involved.

The analysis of the  $m/z = 17$  and 18 channels corresponding to HO<sup>+</sup> and H<sub>2</sub>O<sup>+</sup> respectively is presented Figure 7A and allows to study the becoming of water.

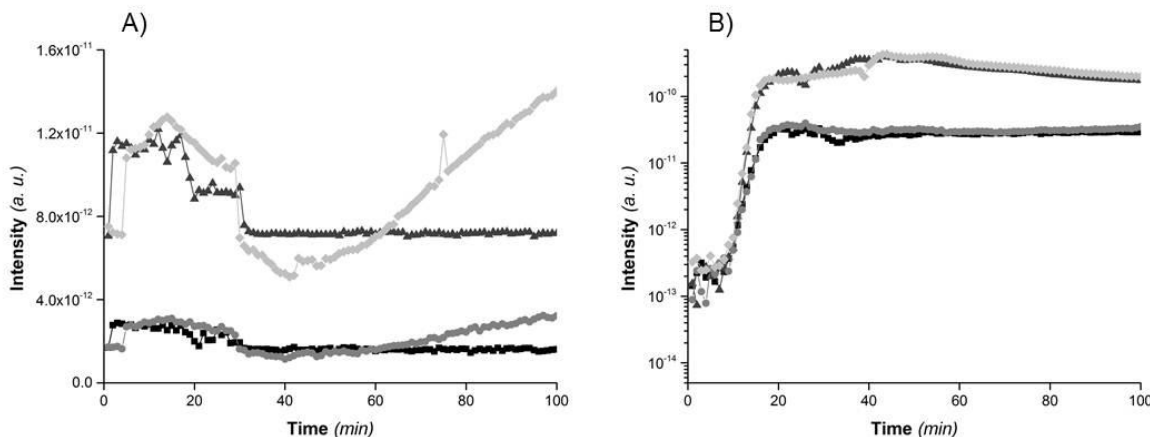


**Figure 7:** A) Evolution of the OH<sup>+</sup> and OH<sub>2</sub><sup>+</sup> fragments (channels 17 and 18) characteristic of H<sub>2</sub>O from EC-LiPF<sub>6</sub> (**■ and ●**) and EC-LiPF<sub>6</sub>-H<sub>2</sub>O (**▲ and ◇**) mixtures.  
 B) Logarithmic evolution of the CO<sub>2</sub><sup>+</sup> fragments (channels 44) characteristic of CO<sub>2</sub> from EC-LiPF<sub>6</sub> (**■**), EC-LiPF<sub>6</sub>-H<sub>2</sub>O (**▲**), LCO (**●**) and LCO-H<sub>2</sub>O (**◇**) systems

The detection of  $\text{HO}^+$  and  $\text{H}_2\text{O}^+$  fragments between 5 and 25 minutes is attributed to the initial introduction of water in the mixture. After its volatilization and/or reaction towards other species, an unexpected formation of *in situ* water occurs after 40 minutes, consecutively to the aforementioned  $\text{OPF}_3$  regeneration.

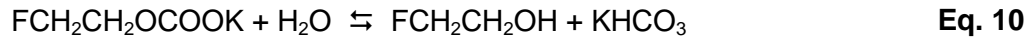
Finally, Figure 7B is used to track the degradation of ethylene carbonate into  $\text{CO}_2$ . It appears that addition of water in the electrolyte promotes the EC degradation, with a huge amount of emitted  $\text{CO}_2$  compared to the electrolyte degradation in dry conditions (maximum intensity is reached around 40 minutes). If water modifies this electrolyte degradation, it is not the case of LCO (equivalent quantities of emitted  $\text{CO}_2$ ). This neutral effect of the positive electrode material in dry or wet conditions on the  $\text{CO}_2$  emission is systematic, whatever the considered material (results not shown).

### **3.4. Modification induced by the simultaneous presence of water and positive electrode material on the decomposition of EC- $\text{LiPF}_6$ electrolyte at 240°C**

The decomposition of the electrolyte at 240°C in presence of water made it possible to evidence two other molecules as potential degradation products.

The first one is 2-fluoroethanol, whose presence also mentioned by Hammami *et al.* [27] is explained by these authors based on the work of Bergmann *et al.* [37].

Bergmann details that ethylene carbonate can react with potassium fluoride in presence of water following eq.9-10:



Considering the work of Bergmann, Hammami *et al.* propose a direct reaction between EC and a fluorinated agent (denoted RF). However, these authors do not give any information about the nature of the RF molecule involved in the reaction. Moreover, the importance of the hydrolysis step is not discussed as they consider as possible the formation of  $\text{FCH}_2\text{CH}_2\text{OH}$  from the reaction between EC and RF. Finally, these authors claims a possible catalytic effect of LCO on the formation of 2-fluoroethanol.

Material impact on the generation of 2-fluoroethanol has been probed and the results obtained with LCO, NMC, LMO and C-LFP in dry and wet conditions are given Figure 8A.

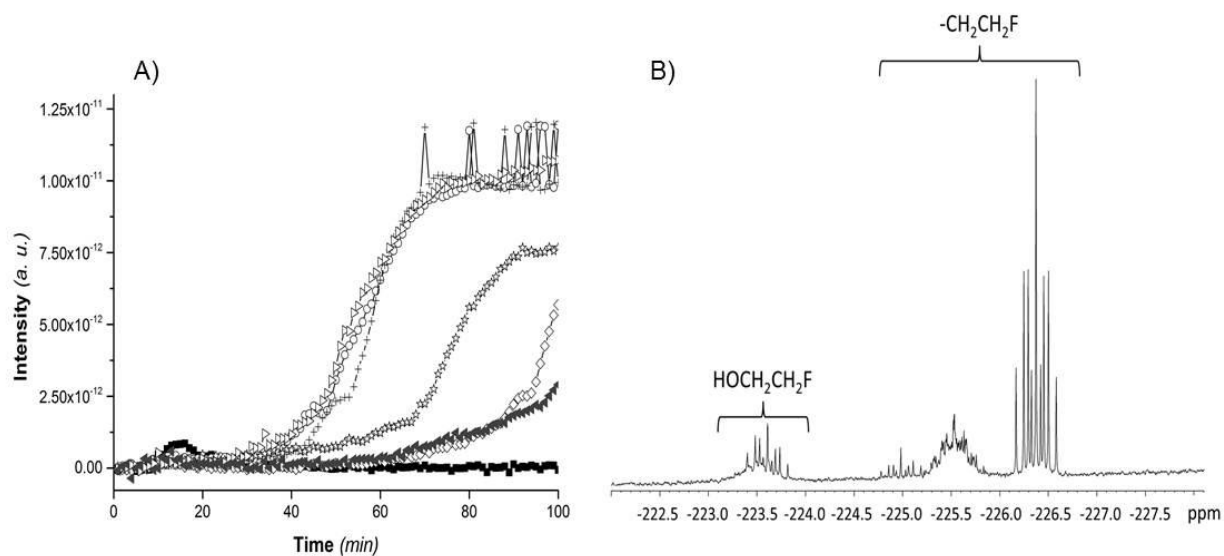


**Figure 8:** A) Evolution of the  $\text{CH}_2\text{OH}^+$  fragment (channel 31) characteristic of 2-fluoroethanol ( $\text{C}_2\text{H}_5\text{OF}$ ) from EC-LiPF<sub>6</sub>(ref) (■), EC-LiPF<sub>6</sub>-H<sub>2</sub>O(○), LCO-H<sub>2</sub>O(+), NMC-H<sub>2</sub>O(◇), LMO-H<sub>2</sub>O(★), C-LFP(◀), C-LFP-H<sub>2</sub>O(▶) systems.  
B) <sup>19</sup>F NMR spectra area of 2-fluoroethanol in EC-LiPF<sub>6</sub>-H<sub>2</sub>O system.

Comparing simplified reference electrolyte in dry and wet conditions, it is only when water is present that the contribution of the  $\text{CH}_2\text{OH}^+$  fragment significantly arises from 40 minutes to reach a maximum after 70 minutes, then remains steady. It means that the formation of 2-fluoroethanol is possible in presence of water, even if no material is present as catalyst. An exception is shown with C-LFP in dry conditions resulting in a slight increase of  $\text{CH}_2\text{OH}^+$  fragment. Complementary studies will be performed to investigate further this exception. In wet conditions every materials react differently.

It is clear that the addition of LCO does not modify the contribution of the  $\text{CH}_2\text{OH}^+$  fragment: LCO does not play a role of catalyst.

On the contrary, the addition of the LMO seems to slow down the F-CH<sub>2</sub>-CH<sub>2</sub>-OH emission during the thermal degradation of simplified reference electrolyte in presence of water. A similar but more significant inhibiting effect is also observed when NMC is present in the mixture. Finally, the presence of C-LFP in wet conditions leads to the same degradation behavior as in wet conditions with or without the presence of LCO implying no catalytic effect.

*Ex situ* <sup>19</sup>F RMN measurements have been performed as complementary experiments to the registration of the m/z = 64 channel (F-CH<sub>2</sub>-CH<sub>2</sub>-OH<sup>+</sup> molecular ion) by mass spectrometry in order to confirm the FCH<sub>2</sub>CH<sub>2</sub>OH formation. The obtained result in wet conditions is presented Figure 8B.

The three signals between -224.5 ppm and -227 ppm are attributed to polymers with different chain lengths. Intensity and number of multiplets differ from dry systems because of the presence of water which accelerates the rate of polymerization. Poorly resolved resonances at -223.5 ppm (<sup>19</sup>F NMR) is attributed by Gnanaraj *et al.* to the presence of -CH<sub>2</sub>CH<sub>2</sub>F fragment of 2-fluoroethanol [11]. These data confirm the formation of 2-fluoroethanol detected in our work by *in situ* mass spectrometry and also mentioned in the literature [27].

The other decomposition product evidenced in this study is 1,4-dioxane also mentioned by Gachot *et al.* [38], even if these authors do not originate it from thermal degradation of EC. Indeed, these authors assume the formation of 1,4-dioxane from the decomposition of DMC, what cannot be observed in our study as the only used carbonate for preparing the simplified reference electrolyte is EC. The detection of relevant variation of channels 57, 58 and 88 is consistent with the molecule 1,4-dioxane. If no formation mechanism for this species can be proposed in the applied thermal conditions without complementary studies, it can be ensured that water is needed to generate 1,4-dioxane (see supplementary materials). This last unexpected result is a supplementary reason which comforts the authors in the fact that the development of such a device of analysis in real time is clearly a nice tool for investigating the complexity of the Li-ion battery chemistry and corresponding degradation mechanisms.

## Conclusion

The study of the interaction between positive electrode materials and electrolyte in dry and wet conditions has been realized by means of real-time mass spectrometry. This analysis allowed to follow gas formation during the degradation of various mixtures at 240°C. Following the evolution of specific gases such as  $\text{OPF}_3$  and  $\text{CO}_2$  confirms well known phenomena like  $\text{LiPF}_6$  hydrolysis or polymerization reactions. It also highlights the formation of rarely discussed species such as 2-fluoroethanol and 1,4-dioxane. It appears that the presence of water or other protic impurities greatly influence their formation. The reliability of this technic has been established and gives first promising results. Thus, addition of component one by one allows to show their role in gas formation during heating. Further studies are contemplated regarding electrode scale which takes into account other component such as black carbon and binder. The role of these compounds will be investigated separately, following an equivalent step-by-step approach.

## Acknowledgements:

The authors wish to express their appreciation to the technical support of Sébastien Leclerc for NMR measurements and Jean-François Marêché for device and discussion as well as to the financial support of ANR-T and Renault Company.

## References

- [1] M. Armand, J.-M. Tarascon, *Nature*, 451 (2008) 652-657.
- [2] D. Aurbach, B. Markovsky, I. Weissman, E. Levia, Y. Ein-Eli, *Electrochim. Acta*, 45 (1999) 67-86.
- [3] D. Lisbona, T. Snee, *Process Saf. Environ. Prot.*, 89 (2011) 434-442.
- [4] Q. Wang, P. Ping, X. Zhao, G. Chub, J. Sun, C. Chen, *J. Power Sources*, 208 (2012) 210-224.
- [5] S. Wilken, M. Treskow, J. Scheers, P. Johansson, P. Jacobsson, *RSC Adv.*, 3 (2013) 16359-16364.
- [6] H. Yang, G. V. Zhuang, P. N. Ross Jr., *J. of Power Sources*, 161 (2006) 573–579.
- [7] E. Zinigrad, L. Larush-Asraf, J. S. Gnanaraj, M. Sprecher, D. Aurbach, *Thermochim. Acta*, 438 (2005) 184-191.
- [8] T. Kawamura, A. Kimura, M. Egashira, S. Okada, J.I. Yamaki, *J. Power Sources*, 104 (2002) 260-264.

- [9] L. Terborg, S. Nowak, S. Passerini, M. Winter, U. Karst , P. R. Haddad, P. N. Nesterenko, *Anal. Chim. Acta*, 714 (2012) 121-126.
- [10] G. G. Botte, R. E. White, Z. Zhang, *J. Power Sources* 97-98 (2001) 570-575.
- [11] J. S. Gnanaraj, E. Zinigrad, L. Asraf, H. E. Gottlieb, M. Sprecher, M. Schmidt, W. Geissler, and D. Aurbach, *J. Electrochem. Soc.*, 150 (2003) A1533-A1537.
- [12] C. Arbizzani, G. Gabrielli, M. Mastragostino, *J. Power Sources*, 196 (2011) 4801-4805.
- [13] A. M. Andersson, M. Herstedt, A. G. Bishop, K. Edström, *Electrochem. Acta*, 47 (2002) 1885-1898.
- [14] B. Ravdel, K.M. Abraham, R. Gitzendanner, J. DiCarlo, B. Lucht, C. Campion, *J. Power Sources*, 119-121 (2003) 805-810.
- [15] L. Terborg, S. Weber, S. Passerini, M. Winter, U. Karst, S. Nowak, *J. Power Sources*, 245 (2014) 836-840.
- [16] S. Wilken, P. Johansson, P. Jacobsson, *Solid State Ionics*, 225 (2012) 608-610.
- [17] C. Campion, W. Li, B. L. Lucht, *J. Electrochem. Soc.*, 152 (2005) A2327-A2334.
- [18] V. Kraft, M. Grützke, W. Weber, M. Winter, S. Nowak, *J. Chromatography A*, 1354 (2014) 92-100.
- [19] L. Terborg, S. Weber, F. Blaske, S. Passerini, M. Winter, U. Katst, S. Nowak, *J. Power Sources*, 242 (2013) 832-837.
- [20] D. Ortiz, V. Steinmetz, D. Durand, S. Legrand, V. Dauvois, P. Maitre, S. Le Caër, *Nature communications*, (2015).
- [21] V. Kraft, W. Weber, M. Grützke, M. Winter, S. Nowak, *RSC Adv.*, 5 (2015) 80150.
- [22] Q. Wang, J. Suna, X. Yao, C. Chen, *Thermochim. Acta*, 437 (2005) 12-16.
- [23] G. G. Eshetu, S. Grugeon, S. Laruelle, S. Boyanov, A. Lecocq, J.-P. Bertrand, G. Marlair, *Phys. Chem. Chem. Phys.*, 15 (2013) 9145-9155.
- [24] D. D MacNeil, Z. Lu, Z. Chen, J. R. Dahn, *J. Power Sources*, 108 (2002) 8-14.
- [25] H. F. Xiang, H. Wang, C. H. Chen, X. W. Ge, S. Guo, J. H. Sunc, W. Q. Hu, *J. Power Sources*, 191 (2009) 575-581.
- [26] P. Ping, Q. Wang, J. Sun, H. Xiang, C. Chen, *J. Electrochem. Soc.*, 157 (2010) A1170-A1176.
- [27] A. Hammami, N. Raymond, M. Armand, *Nature*, 424 (2003) 635-637.
- [28] D. R. Gallus, R. Schmitz, R. Wagner, B. Hoffmann, S. Nowak, I. Cekic-Laskovic, R. W. Schmitz, M. Winter, *Electrochem. Acta*, 134 (2014) 393-398.
- [29] S.F. Lux, I.T. Lucas, E. Pollak, S. Passerini, M. Winter, R. Kostecki, *Electrochem. Commun.*, 14 (2012) 47-50.
- [30] A. Lecocq, G. G. Eshetu, S. Grugeon, N. Martin, S. Laruelle, G. Marlair, *J. Power Sources*, 316 (2016) 197-206.
- [31] D. Aurbach, I. Weissman, A. Zaban, P. Dan, *Electrochim. Acta*, 45 (1999) 1135.
- [32] X.-G. Teng, F.-Q. Li, P.-H. Ma, Q.-D. Ren, S.-Y. Li, *Thermochim. Acta*, 436 (2005) 30-34.
- [33] B. Shvartsev, D. Gelman, I. Komissarov, A. Epshtein, D. Starosvetsky, Y. Ein-Eli, *ChemPhysChem*, 16 (2015) 370-376.
- [34] P. Handel, G. Fauler, K. Kapper, M. Schmuck, C. Stangl, R. Fischer, F. Uhlig, S. Koller, *J. Power Sources*, 267 (2014) 255-259.
- [35] Q. Wang, J. Sun, D. Chen, C. Chen, *J. Alloys Compd.*, 48 (2009) 477-481.

- [36] K. Zaghib, J. Dubé, A. Dallaire, K. Galoustov, A. Guerfi, M. Ramanathan, A. Benmaya, J. Prakash, A. Mauger, C.M. Julien, *J. Power Sources*, 219 (2012) 36-44.
- [37] E. D. Bergmann, I. J. Shahak, *J. Chem. Soc.*, (1966) 899-900.
- [38] G. Gachot, P. Ribière, D. Mathiron, S. Grugéon, M. Armand, J.-B. Leriche, S. Pilard, S. Laruelle, *Anal. Chem.*, 83 (2011) 478-485.